

FedProf: Efficient Federated Learning with Data Representation Profiling

Wentai Wu, Ligang He, Weiwei Lin, Rui Mao, Chenlin Huang and Wei Song

Abstract—Federated Learning (FL) has shown great potential as a privacy-preserving solution to learning from decentralized data which are only accessible locally on end devices (i.e., clients). In many scenarios, however, a large proportion of the clients are probably in possession of low-quality data that are biased, noisy or even irrelevant. As a result, they could significantly slow down the convergence of the global model we aim to build and also compromise its quality. In light of this, we propose *FedProf*, a novel protocol for optimizing FL under such circumstances without breaching data privacy. The key of our approach is using the global model to dynamically profile the latent representations of data (termed representation footprints) on the clients. By matching local footprints on clients against a baseline footprint on the server, we adaptively score each client and adjust its probability of being selected each round so as to mitigate the impact of the clients with low-quality data on the training process. We have conducted extensive experiments on public data sets using various FL settings. The results show that *FedProf* effectively reduces the number of communication rounds and overall time (providing up to 4.5x speedup) for the global model to converge while improving the accuracy of the final global model.

Index Terms—federated learning, neural network, distributed computing, machine learning

I. INTRODUCTION

With the advances in Artificial Intelligence (AI), we are seeing a rapid growth in the number of AI-driven applications as well as the amount of data required to train them. However, a large proportion of data used for machine learning are often generated outside the data centers by distributed resources such as mobile phones and IoT (Internet of Things) devices. The trend is growing and it is predicted that the data generated by IoT devices will account for 75% in 2025 [1]. Under this circumstance, it will be very costly to transmit the data collected by the end devices to a central resource (such as cloud servers) for model training. More importantly, moving the data out of their local devices (e.g., mobile phones) is now restricted by law in many countries, such as the General Data Protection Regulation (GDPR)¹ enforced in EU.

It raises three main challenges to learning from decentralized data: 1) **massive scale**: the data are usually distributed over numerous end devices; 2) **limited communication**: the

device-server communication is expensive and limited in bandwidth; and 3) **non-IID distribution**: local data vary in size and exhibit strong discrepancy in distribution.

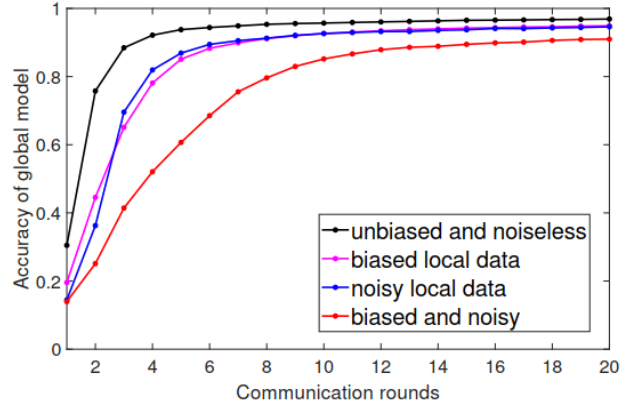


Fig. 1. A demonstration of the global model’s convergence under different data conditions. We ran the FL process with 100 clients to learn a CNN model on the MNIST data set, which is partitioned and allocated to clients in four different ways; 1) *original* (black line): noiseless and evenly distributed over clients, 2) *biased* (magenta line): class-imbalanced local data, 3) *noisy* (blue line): blended with noise, and 4) *biased and noisy* (red line). The noise (if applied) covers 65% of the clients; the dominant class accounts for >50% of the samples for biased local data. The fraction of selected clients is 0.3 each round.

As an emerging paradigm, Federated Learning (FL) [2] is proposed by Google to perform efficient distributed machine learning while protecting the data privacy (i.e., no data exchange). Compared to traditional distributed learning methods, FL adopts a much more efficient communication scheme between end devices (clients) and the server [3][4]. A typical process of FL is organized in rounds. In each round, the clients download the global model from the server, perform local training on their data and then upload their updated local models to the server for aggregation.

A. Motivation

Generally, in each round of FL the server exchanges the model with only a fraction of clients selected for this round of training (involving too many clients leads to diminishing gains for the global model’s quality [22]). The standard FL protocol (i.e., FedAvg [2][5]) selects clients randomly, which implies that every client (and its local data) is considered equally important as they have the same chance of being selected. However, a common problem of decentralized data sources is the **discrepancy in both data quality and data distribution** – a large proportion of on-device data (e.g., user-generated texts

W. Wu, L. He (corresponding author, ligang.he@warwick.ac.uk) are with the Department of Computer Science, the University of Warwick. W. Lin is with the School of Computer Science & Engineering at the South China University of Technology. R. Mao is with the College of Computer Science and Software Engineering, Shenzhen University. C. Huang is with the National University of Defense Technology. W. Song is with the Henan Academy of Big Data, Zhengzhou University.

¹<https://gdpr.eu/what-is-gdpr/>

[8] and photos) can be biased and noisy. In some scenarios, local data may contain irrelevant or even malicious samples [9][10]. In Fig. 1 we demonstrate the impact of involving clients with low-quality data by running FL over 100 clients to learn a CNN model on MNIST using the standard FedAvg protocol. From the traces we can see that training over clients with problematic or strongly biased data can compromise the efficiency and effectiveness of FL, resulting in an inferior global model that takes more rounds to converge. A traditional solution to the problem is local data cleaning and re-sampling [11][12], but in many FL scenarios it may not be feasible to make modifications to users' data or use extra memory/storage space for caching re-sampled and augmented data. Another naive solution is to directly exclude those clients with low quality data, which, however, is often impractical because 1) the quality of data depends on the learning task and is difficult to gauge; 2) some noisy or biased data could be useful to the early-stage training [13]; and 3) sometimes low-quality data are very common across the clients.

B. Contributions

In this paper, we propose a novel scheme called *FedProf* to address the challenges discussed above. We first introduce a data representation profiling method, which uses the global model as a medium and extracts the hidden representation of data from the first fully-connected layer (FC-1). We observed that in the forward propagation, the outputs of each neuron in FC-1 tend to follow the Gaussian distribution. Further, we provide the theoretical proof for this observation, based on which we propose an encoding scheme to convert the representations to a compact format termed *representation footprints*. Next, we present a novel FL protocol that adaptively adjusts each client's chance of participating in each FL round based on the divergence between local footprints (from the clients) and the baseline footprints (on the server). By doing so, the clients with the low-quality data get involved in the training at a reduced rate. Consequently, the convergence of the global model is optimized. We have conducted extensive experiments. The results show that *FedProf* reduces the number of communication rounds by up to 77%, shortens the overall training time (up to 4.5x speedup) while increasing the accuracy of the global model by up to 2.5%.

II. RELATED WORK

Compared with the traditional distributed training methods (e.g., [14][15][16]), Federated Learning assumes the strict constraint of data locality and the limited communication capacity [3]. The original implementation of FL [2][5] adopts a parameter C for controlling the proportion of the clients selected for local training in each FL round, in order to avoid the prohibitive communication costs. It is also suggested that given a large fleet of end devices the fraction C should be carefully limited [6][7].

Much effort has been made in optimizing FL, especially in terms of its efficiency and efficacy. The existing solutions span a variety of perspectives, including optimized communication [3][17][18], model aggregation [21][22], pace steering [4][20],

local training optimization [23][24] and biased client selection [23][27][28]. However, little attention has been paid to the problems caused by the low-quality data on end devices and the challenge of how to minimize their impact on FL's efficiency and effectiveness. Goetz et al. [27] proposed a loss-oriented client selection strategy, in which they prioritize the clients with high loss feedback. This strategy has the tendency to select the clients whose local models yield the higher errors. But it is also likely to favour the clients with noisy and irrelevant data (low quality data). Tuor et al. [24] pointed out that the clients of FL are likely to contain a lot of useless data and only a subset of them is valuable for the training task. They further propose a data selection method based on the loss distribution in order to filter out noisy and irrelevant data on local devices. However, their solution requires a baseline loss distribution produced by a pre-trained model, which could be difficult to set up without the sufficient a priori knowledge. Locally learned representations are very useful for personalized FL [25], which also inspires us to use them as information exchanged between clients and the server for optimized client selection [26].

III. DATA REPRESENTATION PROFILING

In this paper, we consider a typical cross-device FL setting [6], in which multiple end devices perform local training on their data and the server owns a set of benchmark data for evaluation (validation). Local data are bound to and only accessible by the corresponding clients. The benchmark data is used for the round-wise evaluation of the global model and is only accessible by the server.

Assuming n clients, we need some way to profile all local data sets $D_i, i = 1, 2, \dots, n$ and the benchmark data set D^* in order to assess the quality of each local set. The more similar D_i is to D^* in terms of distribution, the more valuable client i is for local training. However, it is usually unrealistic to profile the raw data. On the one hand, the raw feature space such as images can be very high-dimensional and the distribution of samples in each dimension could follow any random pattern, which makes it difficult to profile. On the other hand, the resulting profiles of local data need to be sent to the server for comparison, which could risk leaking user information. Therefore, we propose a novel method that leverages the global model as a medium to profile the *latent representations of data*.

A. Distribution of Representations

In this section we present our profiling method on the basis of latent representations of data from the fully-connected (i.e., dense) layers in the global model. The reasons why we exploit the global model as the medium for data representation profiling are multi-fold. First, introducing a separate data encoder incurs the extra cost in communication and training. Second, once properly initialized hidden layer(s) of the global model can act as a natural encoder that maps the raw data to a set of feature embeddings (i.e., representations), which become more sensitive to the input data of different qualities as the global model improves during the FL process. Besides, the global model is synchronized with the clients every round.

Thus we can guarantee an identical encoder for embedding local data on the clients and the benchmark data on the server.

Our encoding scheme is inspired by an intriguing finding: when we were training a CNN, we recorded the output of every neuron in the dense layers of the model during the forward propagation and observed that the outputs of each neuron (before activation) in the model's first Fully-Connected layer (FC-1) appear to follow the Gaussian distribution. Fig. 2 shows the outputs of several neurons randomly selected from the FC-1 of the CNN model when being trained on MNIST. We can see the distribution of neuron outputs well match the Gaussian distribution since the first epoch of training.

The observation above inspires us to study the distribution of representations from FC-1 in the latent space. Next we provide theoretical proof to support the observation and further present a novel representation encoding method for data representation profiling.

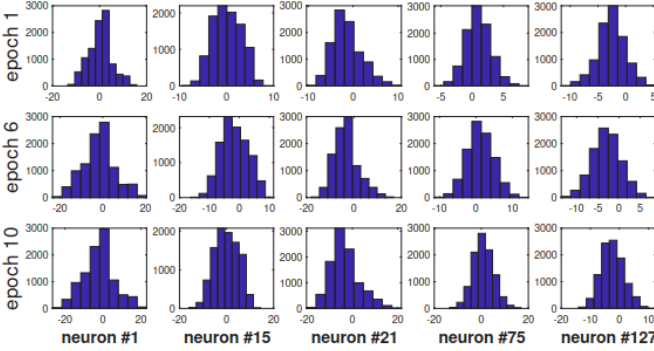


Fig. 2. An example of training LeNet-5 on MNIST for 10 epochs. After each epoch we evaluated the model and collected the un-activated outputs of each neuron in the model's FC-1 layer. Depicted here are the outputs of five randomly selected neurons (namely, #1, #15, #21, #75 and #127 out of 128 neurons in FC-1 for this example) at the epochs 1, 6 and 10.

Let $\Omega = \{neu_1, neu_2, \dots, neu_q\}$ denote the FC-1 of any neural network model (with at least one fully-connected hidden layer) and H_k denote the un-activated output of the neuron neu_k in Ω . We first provide the theoretical proof that H_k should follow the Gaussian distribution in an ideal situation.

Let $\chi : \mathbb{R}^v$ (i.e., v features) denote the input feature set of FC-1 and assume the feature X_i (which is a random variable) follows a certain distribution $\mathcal{F}_i(\mu_i, \sigma_i^2)$ with finite mean $\mu_i = E[X_i]$ and variance $\sigma_i^2 = \text{var}(X_i)$. For each neuron neu_k in the model's FC-1, let $\mathbf{w}_k = [w_1^{(k)} w_2^{(k)} \dots w_v^{(k)}]$ denote the neuron's weight vector (each neuron has v weight components given that the input of the dense layer has v features) and $Z_i^{(k)} = X_i w_i^{(k)}$ denote the i -th weighted input. We make the following assumption:

Assumption 1: The inputs of FC-1 satisfy at least one of the following conditions: 1) X_1, X_2, \dots, X_v are jointly normally distributed. 2) (the Lyapunov's condition) For each neu_k in FC-1, there exists a δ and the weighted inputs $\{Z_i^{(k)}, i = 1, 2, \dots, v\}$ have moments of order $(2 + \delta)$ such that

$$\lim_{v \rightarrow \infty} \frac{1}{s_k^{2+\delta}} \sum_{i=1}^v E \left[|Z_i^{(k)} - w_i^{(k)} \mu_i|^{2+\delta} \right] = 0, \quad (1)$$

where $s_k = \sqrt{\sum_{i=1}^v (w_i^{(k)} \sigma_i)^2}$.

Now we present *Theorem 1*.

Theorem 1: Given a model's FC-1 and a set of inputs that satisfy Assumption 1, the output distribution (during the forward propagation and before activation) of each neuron in FC-1 follows a Gaussian distribution.

Proof. Depending on the conditions stated in Assumption 1, the proof of Theorem 1 is detailed in Appendix A.

Note that Theorem 1 holds as long as one of the two conditions in Assumption 1 is satisfied. In practice, we can generally expect the pattern when the model is properly initialized and the input data are normalized, which is also supported by the observations given in Fig. 2. Next, we discuss our encoding method for representations from FC-1 based on their distribution.

B. Representation Footprints

The representations from the global model's FC-1 can be a profile given a set of data. However, this form of profile is too large in size (which equals to the size of the local data times the number of neurons in FC-1) for efficient information exchange in FL. Based on the insight on FC-1's latent distribution, we use a compact form called *Representation Footprints* to encapsulate data representations. The footprint produced by the FC-1 of the global model w on a data set D , denoted by $FP(w, D)$, is defined by Eq. (2).

$$FP(w, D) = \{(\mu_i, \sigma_i^2) | i = 1, 2, \dots, q\} \quad (2)$$

where the tuple (μ_i, σ_i^2) contains the mean and the variance of the output distribution of the i -th neuron ($i = 1, 2, \dots, q$) in FC-1. The dimension of a footprint is $q \times 2$.

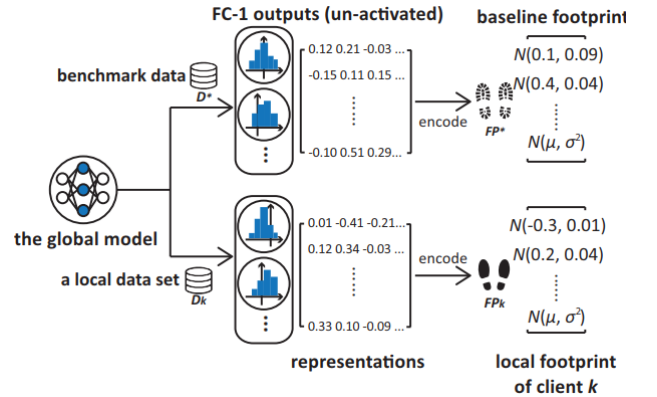


Fig. 3. The proposed representation profiling scheme: the representations of data are encoded as a sequence of (μ_i, σ_i^2) pairs, where μ_i and σ_i^2 are the expectation and the variance, respectively, of the Gaussian distribution of neuron i 's output in FC-1.

Fig. 3 illustrates the workflow of our data representation profiling scheme. The footprints are generated through the model evaluation, the cost of which is marginal compared to that of training the model. The footprints generated for the data on the clients need to be transmitted to the server for comparison with the baseline footprint obtained from the benchmark data on the server. The transmission cost is

negligible since the size of a footprint (as a sequence of (μ, σ^2) pairs) is very small compared to that of the model (note that the model updated by a client each round needs to be uploaded to the server). Let FP_k denote the local footprint from client k , and FP^* denote the baseline footprint in the server. We define the divergence between FP_k and FP^* , denoted by $div(FP_k, FP^*)$, in Eq. (3):

$$div(FP_k, FP^*) = \frac{1}{q} \sum_{i=1}^q \text{KL}(\mathcal{N}_i^{(k)} || \mathcal{N}_i^*), \quad (3)$$

where $\text{KL}(\cdot)$ denotes the Kullback–Leibler (KL) divergence. One advantage of our footprint encoding scheme is that a much simplified KL divergence formula can be adopted because of the Gaussian distribution property of FC-1 latent representations (Appendix B, ref. [30]):

$$\text{KL}(\mathcal{N}_i^{(k)} || \mathcal{N}_i^*) = \log \frac{\sigma_i^*}{\sigma_i^{(k)}} + \frac{(\sigma_i^{(k)})^2 + (\mu_i^{(k)} - \mu_i^*)^2}{2(\sigma_i^*)^2}, \quad (4)$$

With Eq. (4), the KL divergence between two neuron output distributions can be computed without calculating integral or summation, which largely reduces computation cost. Besides, the computation of footprint divergence can be performed under Homomorphic Encryption for minimum knowledge disclosure [33] (see Appendix B for details).

IV. THE FEDPROF TRAINING PROTOCOL

Our research aims to optimize the global model’s convergence in FL over a large group of clients that own the data of diverse quality. Given the client set K ($|K| = n$), let D_k denote the local data set on client k and D^* the benchmark set on the server. To achieve our goal, we need a dynamic client selection strategy $\pi(D_k, D^*, w)$ that serves the optimization problem formulated in (5) where $\rho(D_k, D^*; w)$ differentiates the importance of the local objective functions $F_k(w)$ based on the similarity (in distribution) between D_k and D^* given the current global model w .

$$\arg \min_w F(w) = \sum_{k \in K} \rho(D_k, D^*; w) F_k(w), \quad (5)$$

where w is the parameter set of the global model and $F_k(w)$ is client k ’s local objective function with the loss function $\ell(\cdot)$:

$$F_k(w) = \frac{1}{|D_k|} \sum_{(x_i, y_i) \in D_k} \ell(x_i, y_i; w), \quad (6)$$

The key of our strategy is to rate the quality of the clients’ data in each round and adjust the clients’ chance accordingly in participating in the training. Given the selection fraction C , we use the weighted random selection method² to choose a subset S of $n \cdot C$ participants from K . Let $cred(k)$ denote client k ’s weight in the selection, the value of $cred(k)$ is determined by the divergence between FP_k and FP^* :

$$cred(k) = \exp(-\alpha \cdot div(FP_k(v_k), FP^*(v_k))), \quad (7)$$

where v_k is the version of FP_k (i.e., the version of the global model that client k receives) and α is a preference factor deciding how biased the selection strategy needs to be. The higher the α , the stronger the preference towards the clients with small footprint divergence (i.e., higher data quality). With $\alpha = 0$, our strategy is equivalent to the random selection. In practice, $div(FP_k(v_k), FP^*(v_k))$ is normalized across all footprint divergence values $\{div(FP_j(v_j), FP^*(v_j)) | j = 1, 2, \dots, n\}$.

The processes on clients and the server for our training protocol are detailed in **Algorithm 1**. Note that we only require the selected clients to update and upload local footprints in each round (line 21). Hence, we add an initialization step before the start of the first FL round in order to obtain the initial footprints from clients and initialize $\{cred(k) | k \in K\}$ properly. To do so, the server broadcasts a seed to all the clients for generating an identical initial global model across all clients and generating their first local footprints (line 3). The server needs to take four steps around client selection: 1) Calculates $\{cred(k) | k \in K\}$ according to Eq. (7) (line 8); 2) Selects $n \cdot C$ clients using the weighted random selection function with $cred(k)$ being client k ’s weight (lines 9–10); 3) Collects and updates local footprints from the clients in S (line 15); and 4) Updates the baseline footprint on the server (After global aggregation) (line 18).

The global model $w(t)$ is updated by aggregating local models at the end of round t (line 16). Our protocol supports both full aggregation [2][4] and partial aggregation [22] methods that are adopted in the literature. In the *full aggregation* mode of our protocol, given the selected set of clients in round t (i.e., $S(t)$), the global model is the weighted average across all local models $w_k(t), k = 1, 2, \dots, n$. Note that $\forall k \notin S(t), w_k(t) = w(t-1)$. In the *partial aggregation* mode, only local models from the selected set $S(t)$ contribute to the aggregation. The model aggregation can be formulated as follows:

$$w(t) = \begin{cases} \sum_{k=1}^n \frac{|D_k|}{|D|} w_k(t) & \text{if full aggregation,} \\ \sum_{k \in S(t)} \frac{|D_k|}{|D_{S(t)}|} w_k(t) & \text{if partial aggregation,} \end{cases} \quad (8)$$

where $|D_k|$ is the size of local data set, $|D| = \sum_k |D_k|$ and $|D_{S(t)}| = \sum_{k \in S(t)} |D_k|$.

V. EXPERIMENTS

We have conducted the extensive experiments to evaluate *FedProf* under various FL settings, which cover multiple scales of client population and different machine learning tasks. Apart from the original FL protocol FedAvg [2] proposed by Google, we also reproduced several state-of-the-art FL protocols for comparison. For a fair comparison, the protocols are grouped by the aggregation method (i.e., full aggregation and partial aggregation) and configured with the optimal hyper-parameter values following the settings in their papers (if any). Table I summarizes these FL protocols in terms of their aggregation methods and client selection strategies (the protocols may differ in the specific rules for updating the global model during the aggregation; See the referenced

²For example, using the `random.choices(K, weights, nC)` function provided in the Python Standard Library

Algorithm 1: the FedProf protocol

Input : maximum number of rounds t_{max} , local epochs per round E , client set $K(|K| = n)$, selection fraction C , benchmark data D^* ;

Output: final global model $w(T)$

// Server process: running on the server

- 1 Initializes global model $w(0)$
- 2 $v \leftarrow 0$ // version of the latest global model
- 3 Broadcasts a seed to all clients for model initialization
- 4 Collects initial footprints FP_k from all clients
- 5 $v_k \leftarrow 0 \forall k \in K$
- 6 Generates initial baseline footprint $FP^*(0)$ on D^*
- 7 $n_s \leftarrow C \cdot n$
- for** round $t \leftarrow 1$ to t_{max} **do**
- 8 Calculates $div(FP_k(v_k), FP^*(v_k))$ for each client k
- 9 Updates $\{cred(k)|k \in K\}$ according to Eq. (7)
- 10 $S(t) \leftarrow$ Selects n_s clients based on $\{P(k)|k \in K\}$
- 11 Distributes $w(v)$ to clients in $S(t)$
- 12 **for** client k in $S(t)$ **in parallel do**
- 13 $updateFootprint(k, v)$
- 14 $v_k \leftarrow v \forall k \in S(t)$
- 15 $localTraining(k, t, E)$
- 16 **end**
- 17 Collects local footprints from S
- 18 Updates $w(t)$ according to Eq. (8)
- 19 $v \leftarrow t$
- 20 Evaluates $w(t)$ and generates $FP^*(v)$
- 21 **end**
- 22 **return** $w(T)$

// Client process: running on client k

updateFootprint(k, v):

- 20 Generates $FP_k(v)$ with $w(v)$ on D_k
- 21 Updates footprint $FP_k \leftarrow FP_k(v)$

return

localTraining(k, t, E):

- 22 **for** epoch $e \leftarrow 1$ to E **do**
- 23 Updates $w_k(t)$ using Gradient Descent method
- 24 **end**
- 25 **return**

papers for details). Note that our protocol can adapt to both aggregation methods as indicated by Eq. (8).

In this paper we focus on optimizing the efficiency of FL in terms of the convergence speed and the final quality of the global model. Therefore, we recorded the best accuracy of the global model that each protocol can achieve given a maximum number of rounds, and also compare the protocols in terms of the number of communication rounds, the running time and the energy consumption needed to reach a target accuracy. For brevity, if not specified we report the amount of improvement using FedAvg and FedAvg-RP as the baselines for the full and partial aggregation, respectively.

TABLE I
THE IMPLEMENTED FL PROTOCOLS FOR COMPARISON

Protocol	Aggregation method	Rule of selection
FedAvg [2]	full	random
CFCFM [20]	full	by the order of submission
FedAvg-RP	partial(Scheme II, [22])	random
FedProx [23]	partial	weighted random
FedAdam [21]	partial with momentum	random
AFL [27]	partial with momentum	by the loss on local data
<i>FedProf</i> (ours)	full/partial	by encoded representations

A. Experiment Setup

We built our simulated FL system and implemented the protocols based on the Pytorch framework (Build 1.7.0, CUDA version 10.2.89).

We first set up a Small-scale Task (called S-Task) to learn a regression model from the sensor data, which are distributed over a relatively small number of sources, for predicting the carbon monoxide (CO) and nitrogen oxides (NOx) emissions. Next, we set up a Large-scale Task (called L-Task) to train a global model over a large population of user devices (e.g., smart phones) for the recognition of hand-written digits. In both tasks, each user device possesses the private data and data sharing is not allowed between any parties. We use the *GasTurbine*³ and *EMNIST digits*⁴ data sets for S-Task and L-Task, respectively. The data are non-IID across the end devices⁵. For both tasks, we introduce a diversity of noise into the local data sets on end devices to simulate the discrepancy in data quality.

Detailed experimental settings are listed in Table II. In the S-Task, the total population is 50 and the data collected by a proportion of the sensors (i.e., end devices of this task) are of low-quality: 10% of the sensors have no valid data and 40% of them produce noisy data. In the L-Task, we set up a relatively large population (1000 end devices) and spread the data (from *EMNIST digits*) across the devices with strong class imbalance – on each device, the dominant class accounts for roughly 60% of the samples. Besides, many local data sets are of low-quality: the images on 15% of the clients are irrelevant (valueless for the training of this task), 20% are (Gaussian) blurred, and 25% are affected by the salt-and-pepper noise (random black and white dots on the image, density=0.3). For the S-Task, the maximum number of rounds t_{max} is set to 100 for both aggregation modes, whilst for the L-Task, it is set to 300 and 50 for the full aggregation and partial aggregation, respectively. The preference factor α for our protocol is set to 10. Considering the population of clients, the setting of selection fraction C is based on the suggested scale of training participants in ref. [6].

To simulate a realistic FL system that consists of disparate end devices, the clients are heterogeneous in terms of both performance and communication bandwidth (see Table II). A

³<https://archive.ics.uci.edu/ml/datasets/Gas+Turbine+CO+and+NOx+Emission+Data+Set>

⁴<https://www.nist.gov/itl/products-and-services/emnist-dataset>

⁵In the S-Task, local data sets are of different sizes that follow a Gaussian distribution. In the L-Task, local data are largely imbalanced wherein on each client, roughly 60% of its samples have the same class label.

validation set is kept by the server (as the benchmark data) and used for model evaluation.

TABLE II
EXPERIMENTAL SETUP.

Setting	Symbol	S-Task	L-Task
Model	w	MLP	LeNet-5
Dataset	D	GasTurbine	EMNIST digits
Total size	$ D $	36.7k	280k
Validation set size	$ D^* $	11.0k	40k
Client population	n	50	1000
Data distribution	-	$\mathcal{N}(514, 154^2)$	non-IID, dc0.6
Noise applied	-	fake, gaussian	fake, blur, s&p
Client spec. (GHz)	s_k	$\mathcal{N}(0.5, 0.1^2)$	$\mathcal{N}(1.0, 0.1^2)$
Comm. bandwidth (MHz)	bw_k	$\mathcal{N}(0.5, 0.1^2)$	$\mathcal{N}(1.0, 0.1^2)$
Signal-noise ratio	SNR	1e2	1e2
Bits per sample	BPS	11*8*8	28*28*1*8
Cycles per bit	CPB	300	400
# of local epochs	E	2	5
Loss function	f	MSE Loss	NLL Loss
Learning rate	η	1e-2	1e-2
lr decay	-	0.99	0.99

In each FL round, the server selects a fraction (i.e., C) of clients, distributes the global model to these clients and waits for them to finish the local training and upload the models. Given a selected set of clients $S(t)$, the time duration of an FL round can be formulated as:

$$T_{round} = \max_{k \in S(t)} \{T_k^{comm} + T_k^{train} + T_k^{FP}\} \quad (9)$$

where T_k^{comm} and T_k^{train} are the device-server communication time and local training time, respectively. T_k^{FP} is the time for generating and uploading local footprints (other protocols do not have the term T_k^{FP}).

We assume the wireless communication between the clients and the server. T_k^{comm} can be modeled by Eq. (10) according to ref. [29], where bw_k is the downlink bandwidth of device k (in MHz); SNR is the Signal-to-Noise Ratio of the communication channel, which is set to be constant as the end devices, in general, are coordinated by the base stations for balanced SNR with fairness-based policies; $msize$ is the size of the model; the model upload time is twice as much as that for model download since the uplink bandwidth is set as 50% of the downlink bandwidth.

$$\begin{aligned} T_k^{comm} &= T_k^{upload} + T_k^{download} \\ &= 2 \times T_k^{download} + T_k^{download} \\ &= 3 \times \frac{msize}{bw_k \cdot \log(1 + SNR)}, \end{aligned} \quad (10)$$

The T_k^{train} in Eq. (9) can be modeled by Eq. (11), where s_k is the device performance (in GHz) and the amount of work in local training; the numerator computes the total number of processor cycles required for processing E epochs of local training on D_k .

$$T_k^{train} = \frac{E \cdot |D_k| \cdot BPS \cdot CPB}{s_k}, \quad (11)$$

T_k^{FP} consists of two parts: T_k^{FPgen} for local model evaluation (to generate the footprints of D_k) and T_k^{FPup} for uploading the footprint. T_k^{FP} can be modeled as:

$$\begin{aligned} T_k^{FP} &= T_k^{FPgen} + T_k^{FPup} \\ &= \frac{1}{E} T_k^{train} + \frac{FPsize}{\frac{1}{2}bw_k \cdot \log(1 + SNR)}, \end{aligned} \quad (12)$$

where T_k^{FPgen} is estimated as the time cost of one epoch of local training; T_k^{FPup} is computed in the the similar way as calculating T_k^{comm} in Eq. (10) (the uplink bandwidth is set as one half of the total bw_k); $FPsize$ is the size of a footprint, which equals to $4 \times 2 \times q = 8 \times q$ (four bytes for each floating point number) according to our definition of footprint in Eq. (2).

We model the energy consumption of the end devices in FL by mainly considering the energy consumption of the transmitters for communication (Eq. 13) and on-device computation for local training (Eq. 14). In our protocol, there is an extra energy cost for generating and uploading footprints (Eq. 15).

$$E_k^{comm} = P_{trans} \cdot T_k^{comm} \quad (13)$$

$$E_k^{train} = P_f s_k^3 \cdot T_k^{train} \quad (14)$$

$$E_k^{FP} = P_{trans} \cdot T_k^{FPup} + P_f s_k^3 \cdot T_k^{FPgen}, \quad (15)$$

where $P_f s_k^3$ is a simplified computation power consumption model [34] and P_f is the power of a baseline processor. P_{trans} is the transmitter's power. We set P_{trans} and P_f to 0.5 and 0.7 Watts based on the benchmarking data provided by ref. [35]. Thus the energy consumed by client k to participate in one round of FL is formulated as (E_k^{FP} is only applicable to our protocol):

$$E_k = E_k^{comm} + E_k^{train} + E_k^{FP}. \quad (16)$$

B. Evaluation Results

We evaluate the performance of our *FedProf* protocol in terms of the effectiveness and efficiency in establishing a global model for the two tasks. We also incorporate FedAvg and five other state-of-the-art protocols for comparison (see Table I). The effectiveness of a protocol is measured by the best model accuracy that the protocol can achieve, whilst the efficiency is evaluated by setting an accuracy goal for the convergence of the global model and is assessed from multiple perspectives including the number of rounds needed, the amount of time required and the device energy consumed for achieving the target accuracy. Tables III and IV summarize the results. Figs. 4, 5, 6 and 7 plot the traces of the accuracy in the round-wise evaluation of the global model.

1) *Convergence in different aggregation modes*: We first evaluate the performance of our protocol by comparing the convergence of the global model using different aggregation modes. From Figs. 4, 5, 6 and 7, we observe that partial aggregation facilitates faster convergence of the global model than full aggregation, which is consistent with the observations by [22]. The difference in convergence speed is especially obvious in the L-Task where partial aggregation requires significantly fewer communication rounds to reach 90% accuracy. Our

TABLE III

THE RESULTS OF RUNNING THE S-TASK; THE FL PROCESS FOR THE S-TASK IS RUN IN TWO WAYS: I) RUNNING FOR t_{max} ROUNDS (PLOTING THE BEST ACCURACY ACHIEVED), AND II) RUNNING THE PROCESS UNTIL THE GLOBAL MODEL REACHES THE TARGETED ACCURACY (80% FOR THE S-TASK). THE TESTED PROTOCOLS ARE GROUPED AND COMPARED ACCORDING TO THEIR AGGREGATION METHODS.

Full aggregation								
C=0.2					C=0.3			
Best accuracy	For accuracy@0.8				Best accuracy	For accuracy@0.8		
	Rounds needed	Time (s)	Energy (Wh)			Rounds needed	Time (s)	Energy (Wh)
FedAvg	0.805	56	2869.66	2.87	0.806	52	3160.01	4.12
CFCFM	0.806	39	1230.81	1.61	0.802	42	1495.34	2.91
Ours	0.824	16	803.74	0.80	0.827	12	701.18	0.94

Partial aggregation								
C=0.2					C=0.3			
Best accuracy	For accuracy@0.8				Best accuracy	For accuracy@0.8		
	Rounds needed	Time (s)	Energy (Wh)			Rounds needed	Time (s)	Energy (Wh)
FedAvg-RP	0.819	13	735.48	0.71	0.817	8	466.90	0.64
FedProx	0.821	16	899.93	0.79	0.810	16	841.65	1.08
FedAdam	0.818	8	438.20	0.42	0.819	12	667.00	0.94
AFL	0.816	6	313.81	0.30	0.813	6	298.81	0.42
Ours	0.844	5	283.76	0.27	0.841	4	235.22	0.35

TABLE IV

THE RESULTS OF THE L-TASK; THE FL PROCESS FOR THE L-TASK IS RUN IN TWO WAYS: I) RUNNING FOR t_{max} ROUNDS (PLOTING THE BEST ACCURACY ACHIEVED), AND II) RUNNING THE PROCESS UNTIL THE GLOBAL MODEL REACHES THE TARGETED ACCURACY (0.9 FOR THE L-TASK). THE PROTOCOLS ARE GROUPED AND COMPARED ACCORDING TO THEIR AGGREGATION METHODS.

Full aggregation								
C=0.05					C=0.1			
Best accuracy	For accuracy@0.9				Best accuracy	For accuracy@0.9		
	Rounds needed	Time (s)	Energy (Wh)			Rounds needed	Time (s)	Energy (Wh)
FedAvg	0.906	213	10407.30	60.01	0.929	76	3894.26	43.16
CFCFM	0.923	251	8645.17	61.37	0.932	75	2675.56	37.62
Ours	0.926	98	4846.15	28.22	0.945	45	2295.03	25.98

Partial aggregation								
C=0.05					C=0.1			
Best accuracy	For accuracy@0.9				Best accuracy	For accuracy@0.9		
	Rounds needed	Time (s)	Energy (Wh)			Rounds needed	Time (s)	Energy (Wh)
FedAvg-RP	0.937	12	572.90	3.29	0.938	12	603.94	6.57
FedProx	0.936	13	640.01	3.58	0.942	11	559.16	5.91
FedAdam	0.940	12	599.96	3.47	0.939	12	608.85	6.76
AFL	0.952	10	479.73	2.73	0.944	9	476.62	5.26
Ours	0.962	8	383.94	2.26	0.962	8	413.16	4.64

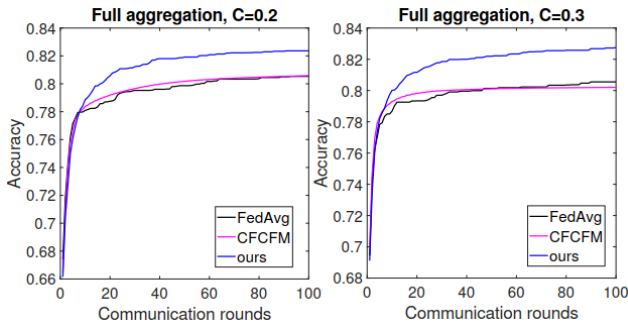


Fig. 4. The traces of evaluation accuracy of the global model through 100 rounds using the full-aggregation protocols in the S-Task.

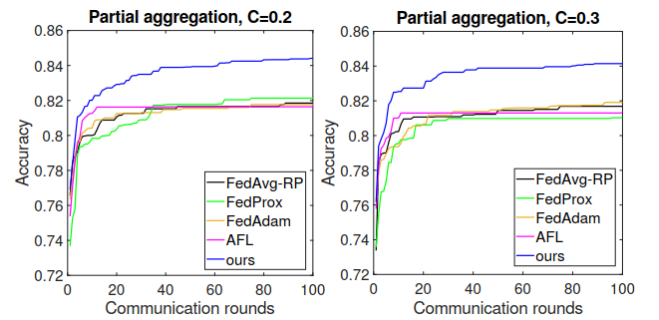


Fig. 5. The traces of evaluation accuracy of the global model through 100 rounds using the partial-aggregation protocols in the S-Task.

FedProf protocol yields the fastest convergence in both groups of comparison for both tasks because limiting the contribution from clients with low-quality data benefits the global model for both aggregation methods.

2) *Best accuracy of the global model*: Through the federated learning process, the global model is evaluated each round on the server. The best global model obtained thus far is kept on the server. In case where the global model obtained in the

current round is inferior to the best one, the inferior model is discarded. In the second column of Tables III and IV we compare the best accuracy the global model can reach given a sufficient number of rounds in training. Our *FedProf* protocol achieves up to 2.5% accuracy improvement when compared against the baselines (FedAvg and FedAvg-RP). The AFL protocol uses a loss-oriented client selection strategy, which shows the closest performance to our protocol in the L-Task

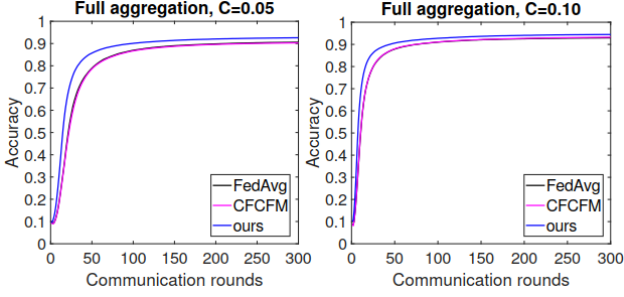


Fig. 6. The traces of evaluation accuracy of the global model through 300 rounds using the full-aggregation protocols in the L-Task.

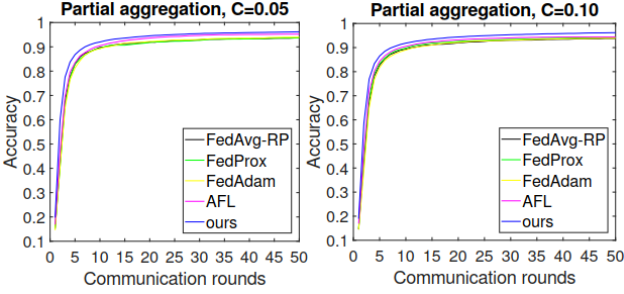


Fig. 7. The traces of evaluation accuracy of the global model through 50 rounds using the partial aggregation protocols in the L-Task.

but the worst accuracy in the S-Task.

3) *Total communication rounds for convergence*: The number of communication rounds required for convergence is a key indicator to the efficiency of FL. We recorded this metric by setting an accuracy objective (0.8 and 0.9 for the S-Task and L-Task, respectively) for the protocols in the training process to compare their efficiency, as summarized in Tables III and IV. In the S-Task, our protocol takes less than half the communication rounds required by other protocols in most cases. In the L-Task, the global model converges slowly using the full aggregation method with $C=0.05$; our protocol reaches 90% accuracy within 100 rounds whilst FedAvg and CFCFM need more than 200. In this case, *FedProf* also achieves approximately 7% higher accuracy at round 50 compared to FedAvg and CFCFM. Partial aggregation methods turn out to be much more efficient in terms of convergence, which also implies significant less communication costs for the global model to converge. FedAvg-RP needs at least 8 rounds to reach the accuracy target for the S-Task and 12 rounds for the L-Task, whilst our protocol reduces the numbers to 5 and 8, respectively.

4) *Total time needed for convergence*: The overall time consumption is tightly coupled with the number of communication rounds for convergence, but it also reflects the actual time cost for each round of training (which includes local training and model transmission). The third column of Tables III and IV gives the total time consumed by each protocol to achieve the preset accuracy of the global model. We can see that protocols requiring more rounds to converge typically take longer to reach the accuracy target except the case of CFCFM, which prioritizes the clients that work faster. Using FedAvg

as the baseline, CFCFM accelerates the training process by 2.1x whilst our protocol provides a 4.5x speedup in terms of achieving the target accuracy (S-Task, $C=0.3$). *FedProf* also has a clear advantage over FedAvg-RP, FedProx and FedAdam in the partial aggregation group where it shows a 2.6x speedup over FedAvg-RP in the S-Task with $C=0.2$.

5) *Device-side energy consumption*: A main concern for the end devices, as the participants of FL, is their power usage in both local training and communication. In this paper we present the analysis from a holistic perspective by evaluating the total energy consumption (in Watt hours) across all of the clients. The results are summarized in Tables III and IV. It is obvious that device-side energy consumption is closely associated to the total number of communication rounds and the total time span until the convergence. Protocols using the full aggregation method have slower convergence and thus generate higher energy cost on the devices. For example, with a small selection fraction $C=0.05$ in the L-Task, FedAvg and CFCFM both consume over 60 Wh to reach the accuracy mark. In this case, our protocol manages to reduce the energy consumption by more than a half (28.22 Wh). With the partial aggregation mode, the total energy consumption is cut down by up to 62% using our protocol (S-Task, $C=0.2$). considering all the cases, our protocol manages to achieve the target accuracy with the least cost, resulting in a reduction of device energy consumption by 29% ~ 53%.

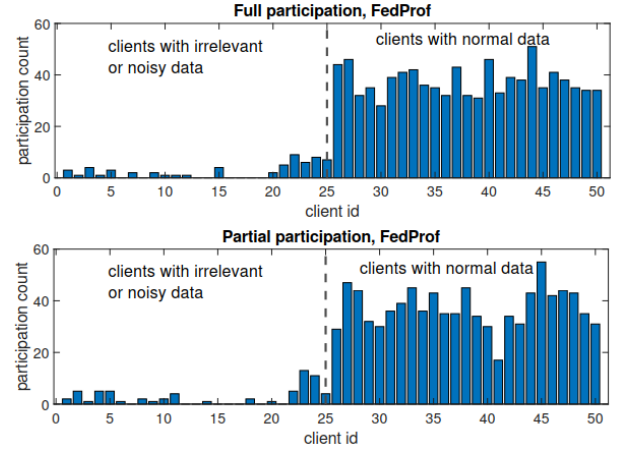


Fig. 8. Total counts by client of participation (i.e., being selected) in S-Task. For clarity, clients are indexed according to their local data quality.

6) *Differentiated participation with FedProf*: Our *FedProf* protocol dynamically adjusts each client's probability of being selected. In this way some clients participate at a largely reduced rate if our algorithm reports a high divergence between their local representation footprints and the baseline footprint, which means that their local data are very likely to be low-quality. Fig. 8 reflects the preference of our selection strategy in S-Task with $C=0.2$; we can observe that clients with useless samples or noisy data get significantly less involved (<10 on average). Fig. 9 gives the participation counts by client in the L-Task. In this task our protocol also effectively limits (basically excludes) the clients who are training on image data of poor quality (i.e., irrelevant or severely blurred), whereas

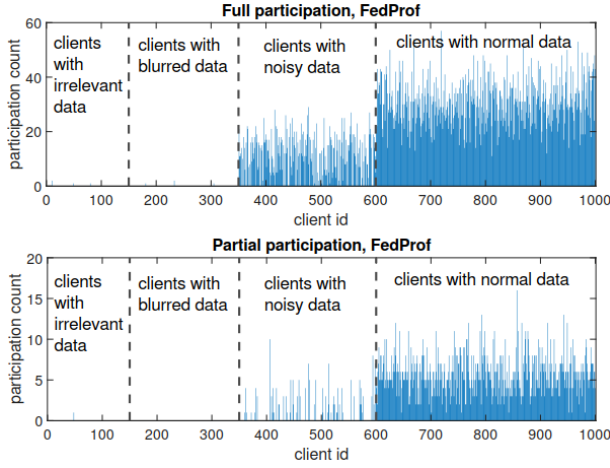


Fig. 9. Total counts by client of participation (i.e., being selected) in L-Task. For clarity, clients are indexed according to their local data quality.

the clients with noisy images (blended with moderate salt-and-pepper noise) are selected at a reduced probability as compared to those with normal data. A potential issue of having the preference towards some of the devices is about fairness. Nonetheless, one can apply our protocol together with an incentive mechanism (e.g., [36]) to address the issue.

VI. CONCLUSION

Federated learning provides a privacy-preserving approach to decentralized training but the low-quality data on end devices could significantly affect the convergence and the quality of the global model we want to build. In this paper, we propose a novel FL protocol *FedProf* to address the issue without violating the data locality restriction of FL. Our basic idea is to discriminate clients by their local data and the key design of our protocol comprises: 1) a dynamic data representation profiling method that generates model-data footprints by encoding the hidden data representation with the global model, and 2) a client selection strategy that adaptively adjusts clients' participating chance based on the divergence between the local footprints from devices and the baseline footprints on the server. Results of comprehensive experiments under various FL settings show that our protocol significantly improves the global model's quality and reduces the costs for the global model's convergence.

The future plan of our study will be focused on methods for optimizing local training by means of acquiring more comprehensive knowledge on local data distribution.

REFERENCES

- [1] Robert van der Meulen. What Edge Computing Means for Infrastructure and Operations Leaders. [Online]. Available: <https://www.gartner.com/smarterwithgartner/what-edge-computing-means-for-infrastructure-and-operations-leaders/>
- [2] McMahan, B., Moore, E., Ramage, D., Hampson, S., & y Arcas, B. A. (2017, April). Communication-efficient learning of deep networks from decentralized data. In *Artificial Intelligence and Statistics* (pp. 1273-1282). PMLR.
- [3] Konečný, J., McMahan, H. B., Yu, F. X., Richtárik, P., Suresh, A. T., & Bacon, D. (2016). Federated learning: Strategies for improving communication efficiency. *arXiv preprint arXiv:1610.05492*.
- [4] Wang, S., Tuor, T., Salonidis, T., Leung, K. K., Makaya, C., He, T., & Chan, K. (2019). Adaptive federated learning in resource constrained edge computing systems. *IEEE Journal on Selected Areas in Communications*, 37(6), 1205-1221.
- [5] Bonawitz, K., Eichner, H., Grieskamp, W., Huba, D., Ingerman, A., Ivanov, V., ... & Roselander, J. (2019). Towards federated learning at scale: System design. *arXiv preprint arXiv:1902.01046*.
- [6] Kairouz, P., McMahan, H. B., Avent, B., Bellet, A., Bennis, M., Bhagoji, A. N., ... & Zhao, S. (2019). Advances and open problems in federated learning. *arXiv preprint arXiv:1912.04977*.
- [7] Wu, W., He, L., Lin, W., & Mao, R. (2020). Accelerating Federated Learning over Reliability-Agnostic Clients in Mobile Edge Computing Systems. *IEEE Transactions on Parallel and Distributed Systems*.
- [8] Hard, A., Rao, K., Mathews, R., Ramaswamy, S., Beaufays, F., Augenstein, S., ... & Ramage, D. (2018). Federated learning for mobile keyboard prediction. *arXiv preprint arXiv:1811.03604*.
- [9] Bhagoji, A. N., Chakraborty, S., Mittal, P., & Calo, S. (2019, May). Analyzing federated learning through an adversarial lens. In *International Conference on Machine Learning* (pp. 634-643). PMLR.
- [10] Bagdasaryan, E., Veit, A., Hua, Y., Estrin, D., & Shmatikov, V. (2020, June). How to backdoor federated learning. In *International Conference on Artificial Intelligence and Statistics* (pp. 2938-2948). PMLR.
- [11] Lin, W. C., Tsai, C. F., Hu, Y. H., & Jhang, J. S. (2017). Clustering-based undersampling in class-imbalanced data. *Information Sciences*, 409, 17-26.
- [12] Cui, Y., Jia, M., Lin, T. Y., Song, Y., & Belongie, S. (2019). Class-balanced loss based on effective number of samples. In *Proceedings of the IEEE/CVF Conference on Computer Vision and Pattern Recognition* (pp. 9268-9277).
- [13] Feelders, A. J. (1996, January). Learning from Biased Data Using Mixture Models. In *KDD* (pp. 102-107).
- [14] Alistarh, D., Grubic, D., Li, J., Tomioka, R., & Vojnovic, M. (2017). QSGD: Communication-efficient SGD via gradient quantization and encoding. In *Advances in Neural Information Processing Systems* (pp. 1709-1720).
- [15] Wu, J., Huang, W., Huang, J., & Zhang, T. (2018, July). Error Compensated Quantized SGD and its Applications to Large-scale Distributed Optimization. In *Proceedings of the International Conference on Machine Learning* (pp. 5321-5329).
- [16] Zheng, S., Meng, Q., Wang, T., Chen, W., Yu, N., Ma, Z. M., & Liu, T. Y. (2017, July). Asynchronous stochastic gradient descent with delay compensation. In *International Conference on Machine Learning* (pp. 4120-4129). PMLR.
- [17] Niknam, S., Dhillon, H. S., & Reed, J. H. (2020). Federated learning for wireless communications: Motivation, opportunities, and challenges. *IEEE Communications Magazine*, 58(6), 46-51.
- [18] Luping, W. A. N. G., Wei, W. A. N. G., & Bo, L. I. (2019, July). Cmf1: Mitigating communication overhead for federated learning. In *2019 IEEE 39th International Conference on Distributed Computing Systems (ICDCS)* (pp. 954-964). IEEE.
- [19] Xie, C., Koyejo, S., & Gupta, I. (2019). Asynchronous federated optimization. In *12th Annual Workshop on Optimization for Machine Learning (OPT2020)*.
- [20] Wu, W., He, L., Lin, W., Mao, R., Maple, C., & Jarvis, S. A. (2020). SAFA: a Semi-Asynchronous Protocol for Fast Federated Learning with Low Overhead. *IEEE Transactions on Computers*.
- [21] Leroy, D., Coucke, A., Lavril, T., Gisselbrecht, T., & Dureau, J. (2019, May). Federated learning for keyword spotting. In *ICASSP 2019-2019 IEEE International Conference on Acoustics, Speech and Signal Processing (ICASSP)* (pp. 6341-6345). IEEE.
- [22] Li, X., Huang, K., Yang, W., Wang, S., & Zhang, Z. (2019). On the convergence of fedavg on non-iid data. *arXiv preprint arXiv:1907.02189*.
- [23] Li, T., Sahu, A. K., Zaheer, M., Sanjabi, M., Talwalkar, A., & Smith, V. (2018). Federated optimization in heterogeneous networks. *arXiv preprint arXiv:1812.06127*.
- [24] Tuor, T., Wang, S., Ko, B. J., Liu, C., & Leung, K. K. Overcoming Noisy and Irrelevant Data in Federated Learning. *arXiv preprint arXiv:2001.08300*.
- [25] Liang, P. P., Liu, T., Ziyin, L., Allen, N. B., Auerbach, R. P., Brent, D., ... & Morency, L. P. (2020). Think locally, act globally: Federated learning with local and global representations. *arXiv preprint arXiv:2001.01523*.
- [26] Tan, A. Z., Yu, H., Cui, L., & Yang, Q. (2021). Towards Personalized Federated Learning. *arXiv preprint arXiv:2103.00710*.
- [27] Goetz, J., Malik, K., Bui, D., Moon, S., Liu, H., & Kumar, A. (2019). Active Federated Learning. *arXiv preprint arXiv:1909.12641*.

- [28] Cho, Y. J., Wang, J., & Joshi, G. (2020). Client Selection in Federated Learning: Convergence Analysis and Power-of-Choice Selection Strategies. arXiv preprint arXiv:2010.01243.
- [29] Tran, N. H., Bao, W., Zomaya, A., Nguyen, M. N., & Hong, C. S. (2019, April). Federated learning over wireless networks: Optimization model design and analysis. In IEEE INFOCOM 2019-IEEE Conference on Computer Communications (pp. 1387-1395). IEEE.
- [30] Roberts, S. J., & Penny, W. D. (2002). Variational Bayes for generalized autoregressive models. IEEE Transactions on Signal Processing, 50(9), 2245-2257.
- [31] Lemons, D. S., & Langevin, P. (2002). An introduction to stochastic processes in physics. The Johns Hopkins University Press, p. 34, ISBN 0-8018-6866-1.
- [32] Billingsley, P. Probability and Measure, 2nd ed. New York: p. 371, Wiley, 1986.
- [33] Gentry, C. (2009, May). Fully homomorphic encryption using ideal lattices. In Proceedings of the forty-first annual ACM symposium on Theory of computing (pp. 169-178).
- [34] Song, J., Li, T., Wang, Z., & Zhu, Z. (2013). Study on energy-consumption regularities of cloud computing systems by a novel evaluation model. Computing, 95(4), 269-287.
- [35] Carroll, A., & Heiser, G. (2010, June). An Analysis of Power Consumption in a Smartphone. In Proceedings of the 2010 USENIX conference on USENIX annual technical conference (pp. 1-14). Boston, MA.
- [36] Yu, H., Liu, Z., Liu, Y., Chen, T., Cong, M., Weng, X., ... & Yang, Q. (2020, February). A fairness-aware incentive scheme for federated learning. In Proceedings of the AAAI/ACM Conference on AI, Ethics, and Society (pp. 393-399).

APPENDIX A PROOF OF THEOREM 1

For each neu_k in the model's FC-1, we have $neu_k = (\mathbf{w}_k, b_k)$ where $\mathbf{w}_k = [w_1^{(k)} w_2^{(k)} \dots]$ is the weight vector and b_k denotes the bias. Let H_k denote the output of neu_k . During the forward propagation, we have:

$$\begin{aligned} H_k &= X \mathbf{w}_k^T + b_k \\ &= \sum_{i=1}^v X_i w_i^{(k)} + b_k \\ &= \sum_{i=1}^v Z_i^{(k)} + b_k \end{aligned} \quad (17)$$

(because $Z_i^{(k)} = X_i w_i^{(k)}$)

Apparently $Z_i^{(k)}$ is a random variable as $Z_i^{(k)} = X_i w_i^{(k)}$ (where the weights $w_i^{(k)}$ are constant during a forward pass), thus H_k is also a random variable according to Eq. (17). Considering the alternative conditions in *Assumption 1*, we discuss the distribution of H_k in two cases.

Case 1. If the first condition in *Assumption 1* is satisfied, the proposed *Theorem 1* automatically holds due to the property of multivariate normal distribution that every linear combination of the components of the random vector $(X_1, X_2, \dots, X_v)^T$ follows a Gaussian distribution [31]. In other words, $H_k = X_1 w_1^{(k)} + X_2 w_2^{(k)} + \dots + X_v w_v^{(k)} + b_k$ is a normally distributed variable since $w_i^{(k)}$ and b_k ($k = 1, 2, \dots, v$) are constants in the forward propagation.

Here we also consider an ideal situation for this case where X_1, X_2, \dots, X_v are independent on each other and X_i follows a Gaussian distribution $\mathcal{N}(\mu_i, \sigma_i^2)$ for all $i = 1, 2, \dots, v$. In this case, by the definition of $Z_i^{(k)}$, we have:

$$Z_i^{(k)} = X_i w_i^{(k)} \sim \mathcal{N}(w_i^{(k)} \mu_i, (w_i^{(k)} \sigma_i)^2), \quad (18)$$

where Z_1, Z_2, \dots, Z_v are independent on each other. Combining Eqs. (17) and (18), we have:

$$H_k \sim \mathcal{N}\left(\sum_{i=1}^v w_i^{(k)} \mu_i + b_k, \sum_{i=1}^v (w_i^{(k)} \sigma_i)^2\right), \quad (19)$$

which proves our *Theorem 1*.

Case 2. In this case we consider a situation where X_1, X_2, \dots, X_v are not necessarily normally distributed but the second condition in *Assumption 1*, i.e., the Lyapunov's condition, is satisfied. As a result, we have the following according to the Central Limit Theorem (CLT) [32] considering that X_i follows $\mathcal{F}_i(\mu_i, \sigma_i^2)$:

$$\frac{1}{s_k} \sum_{i=1}^v (Z_i^{(k)} - w_i^{(k)} \mu_i) \xrightarrow{d} \mathcal{N}(0, 1) \quad (20)$$

where $s_k = \sqrt{\sum_{i=1}^v (w_i^{(k)} \sigma_i)^2}$ and $\mathcal{N}(0, 1)$ denotes the standard normal distribution. Equivalently, for every neu_k we have:

$$\sum_{i=1}^v Z_i^{(k)} \xrightarrow{d} \mathcal{N}\left(\sum_{i=1}^v w_i^{(k)} \mu_i, s_k^2\right) \quad (21)$$

Combining Eqs. (17) and (21) we can derive that:

$$H_k \xrightarrow{d} \mathcal{N}(\sum_{i=1}^v w_i^{(k)} \mu_i + b_k, s_k^2), \quad (22)$$

which means that the output of $neu_k (k = 1, 2, \dots)$ follows Gaussian distribution.

Theoretically, the Lyapunov CLT holds when the weighted inputs $\{Z_i^{(k)} | i = 1, 2, \dots\}$ are pair-wise independent. Nonetheless, FC-1 meets these conditions generally in practice when the model is properly initialized and the input data are normalized, which is also supported by the experimental results shown in Fig. 2. The feature transformation by FC-1 can introduce the correlation to its output and thus the output of the subsequent dense layers after FC-1 may not follow the Gaussian pattern.

APPENDIX B

FOOTPRINT DIVERGENCE UNDER HOMOMORPHIC ENCRYPTION

The proposed footprint matching scheme encodes the latent representations of data into a list of distribution parameters, namely $FP(\mathbf{w}, D) = \{(\mu_i, \sigma_i) | i = 1, 2, \dots, q\}$ where q is the dimension of FC-1. Theoretically, the information leakage (in terms of the data in D) by exposing $FP(\mathbf{w}, D)$ is very limited and it is basically impossible to reconstruct the samples in D given $FP(\mathbf{w}, D)$. Nonetheless, Homomorphic Encryption (HE) can be applied to the footprints (both locally and on the server) so as to guarantee zero knowledge disclosure while still allowing footprint matching under the encryption. In the following we give details on how to encrypt a representation footprint and compute footprint divergence (with decryption) using Homomorphic Encryption (HE).

To calculate (3) and (4) under encryption, a client needs to encrypt (denoted as $[[\cdot]]$) every single μ_i and σ_i^2 in its footprint $FP(\mathbf{w}, D)$ locally before upload whereas the server does the same for its $FP^*(\mathbf{w}, D^*)$. Therefore, according to Eq. (4) we have:

$$\begin{aligned} [[\text{KL}(\mathcal{N}_i^{(k)} || \mathcal{N}_i^*)]] &= \frac{1}{2} \log[[(\sigma_i^*)^2]] - \frac{1}{2} \log[[(\sigma_i^{(k)})^2]] - [[\frac{1}{2}]] \\ &\quad + \frac{([[(\sigma_i^{(k)})^2]] + ([[\mu_i^{(k)}]] - [[\mu_i^*]])^2}{2[[(\sigma_i^*)^2]]}, \end{aligned} \quad (23)$$

where the first two terms on the right-hand side require logarithm operation on the ciphertext. However, this may not be very practical because most HE schemes are designed for basic arithmetic operations on the ciphertext. Thus we also consider the situation where HE scheme at hand only provides *additive and multiplicative* homomorphisms [33]. In this case, to avoid the logarithm operation, the client needs to keep every σ_i^2 in $FP^*(\mathbf{w}, D_i)$ as plaintext and only encrypts μ_i , likewise for the server. As a result, the KL divergence can be computed under encryption as:

$$\begin{aligned} [[\text{KL}(\mathcal{N}_i^{(k)} || \mathcal{N}_i^*)]] &= \left[\left[\frac{1}{2} \log\left(\frac{\sigma_i^*}{\sigma_i^{(k)}}\right)^2 + \frac{1}{2} \left(\frac{\sigma_i^{(k)}}{\sigma_i^*}\right)^2 - \frac{1}{2} \right] \right] \\ &\quad + \frac{1}{2(\sigma_i^*)^2} ([[\mu_i^{(k)}]] - [[\mu_i^*]])^2 \end{aligned} \quad (24)$$

where the first term on the right-hand side is encrypted after calculation with plaintext values $(\sigma_i^{(k)})^2$ and $(\sigma^*)^2$ whereas the second term requires multiple operations based on the ciphertext values $[[\mu_i^{(k)}]]$ and $[[\mu^*]]$.

Now, in either case, we can compute footprint divergence under encryption according to Eq. (3):

$$[[div(FP_k, FP^*)]] = \frac{1}{q} \sum_{i=1}^q [[\text{KL}(\mathcal{N}_i^{(k)} || \mathcal{N}_i^*)]] \quad (25)$$